Triboelectric Nanosensors

DOI: 10.1002/anie.201300437

A Self-Powered Triboelectric Nanosensor for Mercury Ion Detection**

*Zong-Hong Lin, Guang Zhu, Yu Sheng Zhou, Ya Yang, Peng Bai, Jun Chen, and Zhong Lin Wang**

Mercury is a highly toxic metal that can pose serious dangers to the environment and human health. Therefore, monitoring the mercury concentration is an extremely important issue to prevent such a toxic metal from endangering human life.[1] Hg^{2+} ions are by far the most stable inorganic form of mercury, which are non-biodegradable and bioaccumulable. Even at a very low concentrations, they can still be fatal to human brain, heart, and kidney.[2] Multiple approaches, such as atomic absorption/emission spectrometry[3] and inductively coupled plasma mass spectrometry (ICP-MS),[4] have been applied to detect the Hg^{2+} ions in environmental and biological samples. Among these approaches, ICP-MS is the method that has the highest sensitivity and the widest linear range. However, sample preparation before measurement is rather complicated and time-consuming, and requires expensive instrumentation and the use of noble gas. Another drawback of this method is the difficulty in performing in-field analysis. In consideration of the above disadvantages, researchers have instead developed a number of optical methods (colorimetric[5,6] or fluorometric assays,[7–9] and systems based on surface plasmon resonance[10] or surface-enhanced Raman scattering[11]) and electrochemical sensors[12,13] for the detection of Hg^{2+} ions. Optical approaches are advantageous in high sensitivity and selectivity, and practicable for in-field analysis, yet they are involved with sophisticated chemistry in incorporating organic probes, such as crown ethers, porphyrins, specific proteins, DNA, and polymers, which substantially limits their application range.

To overcome the limitations of these methods, the concept of self-powered nanosensors has recently been proposed and tested for its potential toward toxic pollutant detection.[14,15] The working principle of self-powered nanosensors is based on combining/integrating nanogenerators with sensors. The nanogenerators harvest energy from the environment[16–19] to power the sensors. Owing to its convenient monitoring mechanism, the self-powered nanosensors could be the most desirable and promising prototype for environmental protection/detection in the near future because no battery is needed to power the device. For the time being, the major challenge is how to develop a fully integrated, stand-alone and self-powered nanosensor.

The triboelectric effect is an old but well-known phenomenon in daily life. Recently, it has been utilized as an effective way to harvest mechanical energy.[20] Contact between two materials with different triboelectric polarity yields surface charge transfer. The periodic contact and separation of the oppositely charged surfaces can create a dipole layer and a potential drop, which drives the flow of electrons through an external load in responding to the mechanical agitation. As for triboelectric nanogenerator (TENG), maximizing the charge generation on opposite sides can be achieved by selecting the materials with the largest difference in the ability to attract electrons[21] and changing the surface morphology.[22] For the plate-structured TENG, it needs more time and stronger applied force to ensure the contact and separation of the two oppositely charged material surfaces upon pressing and releasing are complete, especially under the electrostatic attraction between them. Adding spacers between two plates[23] or using arch-shaped substrates[24] have been demonstrated to improve the output of TENG.

Herein, we show that the principle of the TENG can be used as a sensor for the detection of Hg^{2+} ions. The first step is to improve the performance of the TENG through the assembly of Au nanoparticles (NPs) onto the metal plate. These assembled Au NPs not only act as steady gaps between the two plates at the strain-free condition, but also enable the function of enlarging the contact area of the two plates, which will increase the electrical output of the TENG. Through further modification of 3-mercaptopropionic acid (3-MPA) molecules on the assembled Au NPs, the high-output nanogenerator can become a highly sensitive and selective nanosensor toward Hg^{2+} ions detection because of the different triboelectric polarity of Au NPs and Hg^{2+} ions. On the basis of this unique structure, the output voltage and current of the triboelectric nanosensor (TENG) reached 105 V and 63 μA with an effective dimension of 1 cm × 1 cm. Under optimum conditions, this TENG is selective for the detection of Hg^{2+} ions, with a detection limit of 30 nM and linear range from 100 nM to 5 μM. A commercial LED lamp was tested as the indicator to replace the expensive electrometer and showed the possibility to simplify the detection system. Our study demonstrates an innovative and unique approach toward self-powered detection of Hg^{2+}.

[*] Dr. Z.-H. Lin,[+] G. Zhu,[+] Y. S. Zhou, Dr. Y. Yang, P. Bai, J. Chen, Prof. Z. L. Wang
School of Material Science and Engineering
Georgia Institute of Technology, Atlanta, GA 30332-0245 (USA)
E-mail: zlwang@gatech.edu
Prof. Z. L. Wang
Beijing Institute of Nanoenergy and Nanosystems
Chinese Academy of Sciences, Beijing (China)

[+] These authors contributed equally to this work.

[**] This work was supported by the U.S. Air Force, MURI, U.S. Department of Energy, Office of Basic Energy Sciences (DE-FG02-07ER46394), NSF, Taiwan (NSC 101-2917-I-564-029), and the Knowledge Innovation Program of the Chinese Academy of Sciences (KJCX2-YW-M13).

Supporting information for this article is available on the WWW under http://dx.doi.org/10.1002/anie.201300437.

The TENG has a layered structure based on two plates (Figure 1a). Glass was selected as the substrate material owing to its strength, light weight, and low cost. On the lower side, the metal plate is prepared. The metal plate consists of

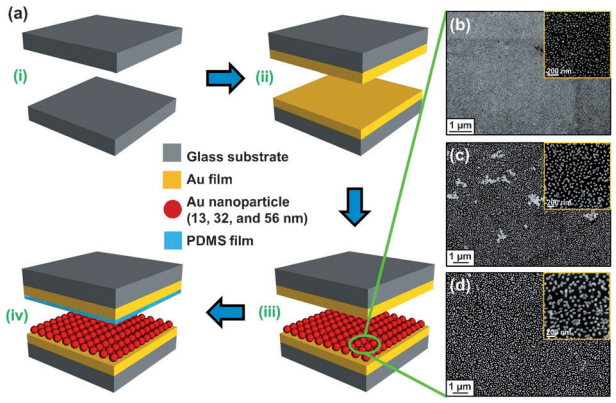

Figure 1. a) Fabrication process of the triboelectric nanogenerator (TENG). b)–d) SEM images of the Au film modified with b) 13 nm, c) 32 nm, and d) 56 nm Au NPs. The TENG has an effective dimension of 1 cm × 1 cm. Scale bars: b)–d) 1 μm; insets: 200 nm.

an Au thin film and assembled Au NPs, which plays dual roles of electrode and contact material. By utilizing 1,3-propanedithiol as the linker molecules, 13 nm, 32 nm, and 56 nm Au NPs were uniformly assembled onto the surface of Au film (Figure 1b–d). Au NPs were prepared by the reduction of Au^{3+} ions with sodium citrate, which also acted as a capping agent to stabilize the as-prepared Au NPs. By carefully controlling the amount of sodium citrate in the synthesis process, different sized Au NPs were synthesized.[25] The UV/Vis absorption spectra display maximum wavelengths of the surface plasmon resonance (SPR) bands of the 13 nm, 32 nm, and 56 nm Au NPs at 519, 528, and 545 nm, respectively (Supporting Information, Figure S1). Compared with other metal NPs, Au NPs feature greater long-term stability and modifiable surface chemistry,[26] and can be synthesized with narrower size distributions.[27,28] For the purpose of selective detection of Hg^{2+} ions, 3-MPA is self-assembled onto the surface of Au NPs through strong Au–S interactions, and its recognition toward Hg^{2+} ions induces Hg^{2+} ions to selectively bind to the Au NP surface.[29,30] On the other plate, another Au thin film is laminated between the glass substrate and a layer of polydimethylsiloxane (PDMS). PDMS is purposely chosen for its advantages of flat surface and easy processing. In this designed device, PDMS and Au are extremely different in their ability to attract and retain electrons in the triboelectric series and can achieve the best results.[31]

The working mechanism of TENG can be explained by the coupling between triboelectric effect and electrostatic effect (Figure 2; glass substrates are not shown for simplification). At the original state before the contact of the two plates (Figure 2a), there is no charge transferred, and thus no electric potential. When an external force is applied on one of the substrates, the Au plate and PDMS plate are brought into contact, which results in electron transfer from a material in the positive side of the triboelectric series to the one in the

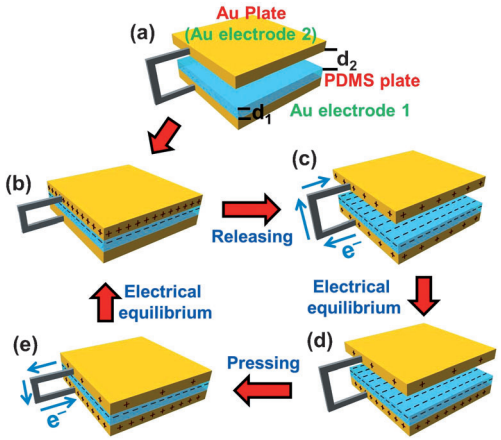

Figure 2. Working mechanism of the TENG. a) Original status without applied force. b) An applied force brings the Au plate and PDMS plate to contact, with the triboelectric effect generating positive charges on the Au plate and negative charges on the PDMS plate. c) Withdrawal of the applied force causes a separation of the charged plates. Potential difference drives electrons from the Au electrode 1 to the Au electrode 2. d) TENG after the screening of triboelectric charges caused by the release step and leaving behind some residual charges to balance the potential difference. e) Electrons are driven from electrode 2 back to Au electrode 1 as the two plates are in contact again.

relatively negative side in the series.[28] Accordingly, electrons are injected from Au electrode 2 onto the PDMS plate, leaving positive charges on the Au plate (Figure 2b). As the force is withdrawn, the contacting surfaces is separated, the Au electrode 2 has a higher potential than the Au electrode 1 at the bottom beneath the PDMS layer, and thus electrons would transfer from the Au electrode 1 to the Au electrode 2 to neutralize the positive triboelectric charges in the Au electrode 2 to reach an electrostatic equilibrium (Figure 2c). This is the first half of the electricity generation process.

In principle, the TENG can be regarded as a flat-panel capacitor. We assume the charge on PDMS is Q, the charge on Au electrode 1 (contact with PDMS) is Q_1, and the charges on Au electrode 2 (Au plate) is Q_2. Based on electrostatic induction and conservation of charges, $-Q = Q_1 + Q_2$. If σ is the charge density on PDMS surface and σ_1 is the charge density of Au electrode 1, we have:[32]

$$\sigma_1 = -\frac{\sigma}{1 + d_1/d_2\varepsilon_{rp}} \quad (1)$$

where ε_{rp} is the relative permittivity of PDMS, d_1 is the thickness of PDMS film, and d_2 is the distance between the two plates. Because d_1 and ε_{rp} are the constant values of 10 μm and about 2.6,[24] respectively, and charge Q is stable for a relatively long time on the PDMS surface, and therefore σ_1 is determined by the gap distance d_2. The variation of d_2 will result in the redistribution of the charges between Au electrode 1 and Au electrode 2 through the external load, and finally reaches a new equilibrium (Figure 2d), which is the experimentally observed electric current. Once the TENG is pressed again, a reduction of the distance d_2 will make the decrease of σ_1, which means that through the

external load the electrons would flow from Au electrode 2 and screen the positive triboelectric charges on the Au electrode 1 (Figure 2e), until reaching a new equilibrium (Figure 2b), which is the second half-cycle of electricity generation. In our experiments, the maximum distance d_2 of the TENG is set up to be 30 mm.

The typical electrical output of the TENG is shown in Figure 3. The TENG was mechanically triggered by a linear motor that provided dynamic impact with controlled force (50 N) at a frequency of 5 Hz, which was monitored by a force sensor (Figure 3a). The electrical output of the TENG greatly depends on the applied force, yielding higher output with larger force (Supporting Information, Figure S2). This is because the two plates are not completely flat, and a larger applied force will contribute more contact area.[20b] The applied force-dependent contact area are shown in the Supporting Information, Figure S3. At a small applied force, the surface roughness prevents fully intimate contact between the Au plate and the PDMS plate. With a larger force, the PDMS can deform owing to its elastic property and fill more vacant space, thus leading to larger contact area. As a result, the electrical output of TENG increases until all the vacant spacing is completely filled by the PDMS, reaching a saturated limit.

Besides, we also compared the electrical output of TENG with different sizes (0.5 cm × 0.5 cm and 1.5 cm × 1.5 cm; Supporting Information, Figure S4) and the TENG with larger size can provide stronger output. This can be explained that the larger contact area yields more surface charge transfer and hence increase the electrical output of TENG. However, by considering the cost efficiency and electrical output of each TENG, we choose the TENG with an effective dimension of 1 cm × 1 cm.

The open-circuit voltage (V_{oc}) and short-circuit current density (J_{sc}) were measured to characterize the electrical performance of as-developed TENG. From Figure 3b, when the Au plate modified with 56 nm Au NPs is connected to the positive probe of the electrometer, upon the release of the pressing force, a positive voltage of 105 V is generated because of the immediate charge separation. As in an open-circuit condition the electrons cannot flow to screen the induced potential difference between the two plates, the voltage will hold at a plateau until the subsequent pressing deformation in the second half cycle. As shown in Figure 3c, the peak value of J_{SC} reaches 63 μA cm^{-2}, corresponding to the half cycle of pressing that is at a higher straining rate than releasing. The integration of each current peak gives the total charges transferred in a half cycle of deformation. We also measured the electrical output of the TENG with a reverse connection to the electrometer. The generated V_{oc} (Figure 3d) and J_{sc} (Figure 3e) showed the corresponding opposite values in Figure 3b and d, indicating that the measured signals were generated by the TENG. The experimental data validate the working mechanism described in Figure 2. The gap and enlarged contact area from the assembled Au NPs are the key factors for the enhanced electrical output. Figure 3f displays the electrical performance of TENG modified with three different sizes of Au NPs (13, 32, and 56 nm). The decreasing order of the generated electrical output is TENG modified with 56 nm Au NPs > TENG modified with 32 nm Au NPs > TENG modified with 13 nm Au NPs > TENG without Au NP modification (bare Au film). The TENG modified with 56 nm Au NPs provided 6.8 times higher J_{sc} and 5.09 times higher V_{oc} than the TENG without Au NP modification. This is because similar density of different-sized

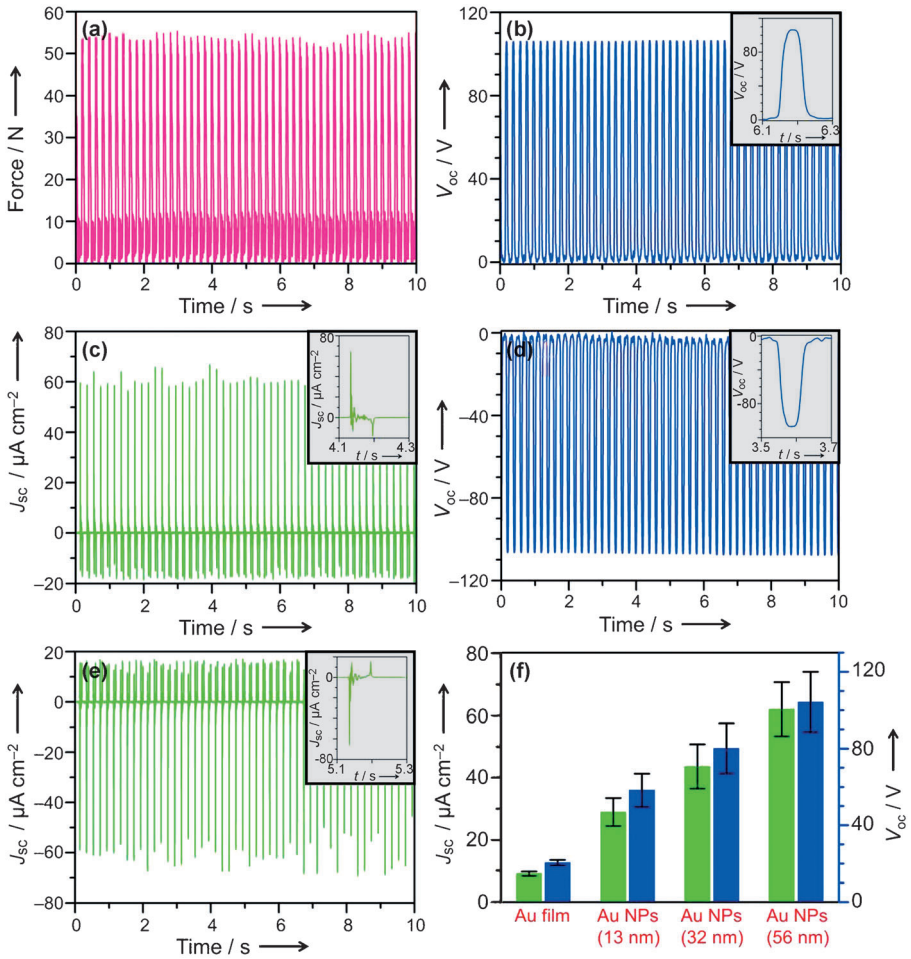

Figure 3. a) Effect of the applied force impacting on the 56 nm Au NP-modified TENG. b)–e) The generated V_{oc} and current density J_{sc} of the 56 nm Au NP-modified TENG at forward connection (b,c) and reversed connection (d,e) to the measurement system. Insets of (b)–(e): enlarged view of one cycle. f) The generated V_{oc} and J_{sc} of different-sized Au NP-modified TENG.

Au NPs on the Au film result in the TENG modified with 56 nm Au NPs providing larger contact area than the others. The density of Au NPs can be varied by controlling the reaction time of Au NPs and 1,3-propanedithiol-modified Au film surface. The lower density of Au NPs decreases the electrical output of TENG (Supporting Information, Figure S5), which also verifies that the electrical output is highly related to the contact area of the two plates. However, when the reaction time is over 12 h, there will exist a non-single Au NP adsorption layer and cause unstable electrical output. Thus we chose the reaction time of 12 h to obtain the densest Au NPs on Au film.

We now demonstrate TENG as a self-powered device for detecting molecular species. Figure 4a shows the output of the TENG by using a full-wave rectifying bridge. For the selective detection of Hg^{2+} ions, Tris-borate (50 mM, pH 9) was used as the buffer solution. The Au plate was soaked with the buffer solution containing various concentrations of Hg^{2+} ions and other metal ions at ambient temperature. The reaction time was optimized to 60 min (Supporting Information, Figure S6). The Au plate was then washed with water and dried at ambient temperature prior to electrical measurement. After the interaction with Hg^{2+} ions (5 μM), the generated J_{sc} of TENG decreased from 63 μA cm^{-2} to 8 μA cm^{-2} (Figure 4b). This is because that the adsorbed molecular species modify the surface triboelectric behavior, by which we can detect the concentration of the Hg^{2+}. By observing TENG performance with an LED lamp, we could build a fully stand-alone and self-powered environmental sensing device. The inset in Figure 4b shows the LED lamp was completely extinguished when detecting the Hg^{2+} ions (5 μM). As a proof of concept, we demonstrated the TENG with the capability to be an environmental sensor without any supporting equipment (power source, capacitor, and electrometer).

Figure 4c shows that the electrical signal of the TENG decreased upon increasing the concentration of Hg^{2+} ions, with a linear relationship between the short-circuit current ratio ($(I_0-I)/I_0$) and the concentration of Hg^{2+} ions ranging from 100 nM to 5 μM ($R^2=0.98$). This approach provides a detection limit at an S/N of 3 at 30 nM for Hg^{2+} ions. Control experiments were carried out to test the selectivity of the developed system toward Hg^{2+} ion detection as compared to other metal ions (each at a concentration of 5 μM). The results displayed in Figure 4d reveal that the sensing system is specific to Hg^{2+} ions, mainly because in comparison to Au NPs, the Hg^{2+} ions have lower tendency to transfer the electrons to PDMS.[33] The high selectivity of 3-MPA toward Hg^{2+} ions resulted from the carboxylic acid, which has much higher binding affinity towards Hg^{2+} ions among all metal ions ($\log\beta_4=17.6$).[34] The potential interference metal ions could not bind to 3-MPA-modified Au NPs, resulting in negligible changes in the electrical signal of the TENG.

In summary, we demonstrated the first triboelectric effect-based sensor for the detection of Hg^{2+} ions by using 3-MPA-modified Au NPs as electrical performance enhancer and recognition element. Based on the high power density (6.9 mW cm^{-2}) of the as-developed TENG, a commercial LED lamp can be used as an indicator instead of expensive electrometers. This novel TENG is quite sensitive (detection limit of 30 nM and linear range of 100 nM–5 μM) and selective for the detection of Hg^{2+} ions. With its high sensitivity, selectivity and simplicity, the TENG holds great potential for the determination of Hg^{2+} ions in environmental samples. The TENG is a future sensing system for unreachable and access-denied extreme environments. As different ions, molecules, and materials have their unique triboelectric polarities, we expect the TENG can become either an electrical turn-on or turn-off sensor when the analytes are selectively binding to the modified electrode surface. We believe this work will serve as the stepping stone for related TENG studies and inspire the development of TENG toward other metal ions and biomolecules,[35] such as DNA and proteins, in the near future.

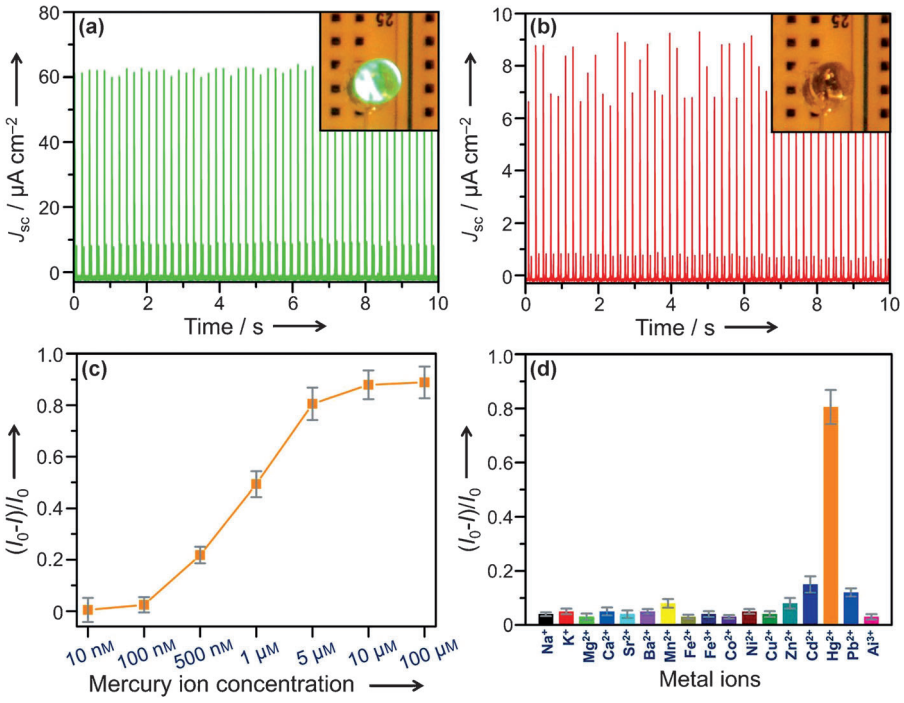

Figure 4. a,b) Rectified J_{sc} of the as-developed TENG before (a) and after (b) the interaction with 5 μM Hg^{2+} ions. Insets: photograph of the indicated LED lamp before (a) and after (b) interaction with 5 μM Hg^{2+} ions, as an indication of detected concentration. c) Sensitivity and d) selectivity of the as-developed TENG for the detection of Hg^{2+} ions. The concentration of all metal ions tested in the selectivity experiment was 5 μM.

Received: January 17, 2013
Revised: February 15, 2013
Published online: ■■ ■■, ■■■■

Keywords: gold nanoparticles · mercury · nanogenerators · self-powered nanosensors · triboelectric effect

[1] T. W. Clarkson, L. Magos, G. J. Myers, *N. Engl. J. Med.* **2003**, *349*, 1731 – 1737.

[2] F. Zahir, S. J. Rizwi, S. K. Haq, R. H. Khan, *Environ. Toxicol. Pharmacol.* **2005**, *20*, 351 – 360.

[3] C. P. Hanna, J. F. Tyson, S. McIntosh, *Anal. Chem.* **1993**, *65*, 653 – 656.

[4] M. Leermakers, W. Baeyens, P. Quevauviller, M. Horvat, *TrAC Trends Anal. Chem.* **2005**, *24*, 383 – 393.

[5] J. S. Lee, M. S. Han, C. A. Mirkin, *Angew. Chem.* **2007**, *119*, 4171 – 4174; *Angew. Chem. Int. Ed.* **2007**, *46*, 4093 – 4096.

[6] M.-L. Ho, K.-Y. Chen, L.-C. Wu, J.-Y. Shen, G.-H. Lee, M.-J. Ko, C.-C. Wang, J.-F. Lee, P.-T. Chou, *Chem. Commun.* **2008**, 2438 – 2440.

[7] S. Yoon, E. W. Miller, Q. He, P. H. Do, C. J. Chang, *Angew. Chem.* **2007**, *119*, 6778 – 6781; *Angew. Chem. Int. Ed.* **2007**, *46*, 6658 – 6661.

[8] C.-C. Huang, Z. Yang, K.-H. Lee, H.-T. Chang, *Angew. Chem.* **2007**, *119*, 6948 – 6952; *Angew. Chem. Int. Ed.* **2007**, *46*, 6824 – 6828.

[9] Z. Gu, M. Zhao, Y. Sheng, L. A. Bentolila, Y. Tang, *Anal. Chem.* **2011**, *83*, 2324 – 2329.

[10] a) D. Li, A. Wieckowska, I. Willner, *Angew. Chem.* **2008**, *120*, 3991 – 3995; *Angew. Chem. Int. Ed.* **2008**, *47*, 3927 – 3931; b) C. Díez-Gil, R. Martínez, I. Ratera, T. Hirsh, A. Espinosa, A. Tárraga, P. Molina, O. S. Wolfbeis, J. Veciana, *Chem. Commun.* **2011**, *47*, 1842 – 1844.

[11] T. Senapati, D. Senapati, A. K. Singh, Z. Fan, R. Kanchanapally, P. C. Ray, *Chem. Commun.* **2011**, *47*, 10326 – 10328.

[12] Z. Zhu, Y. Su, J. Li, D. Li, J. Zhang, S. Song, Y. Zhao, G. Li, C. Fan, *Anal. Chem.* **2009**, *81*, 7660 – 7666.

[13] D. Wen, L. Deng, S. Guo, S. Dong, *Anal. Chem.* **2011**, *83*, 3968 – 3972.

[14] M. Lee, J. Bae, J. Lee, C.-S. Lee, S. Hong, Z. L. Wang, *Energy Environ. Sci.* **2011**, *4*, 3359 – 3363.

[15] I. F. Akyildiz, J. M. Jornet, *Nano Commun. Networks* **2010**, *1*, 3 – 19.

[16] Z. L. Wang, *Adv. Mater.* **2012**, *24*, 280 – 285.

[17] Z. L. Wang, *Sci. Am.* **2008**, *298*, 82 – 87.

[18] B. Tian, X. Zheng, T. J. Kempa, Y. Fang, N. Yu, G. Yu, J. Huang, C. M. Lieber, *Nature* **2007**, *449*, 885 – 890.

[19] Z.-H. Lin, Y. Yang, J. M. Wu, Y. Liu, F. Zhang, Z. L. Wang, *J. Phys. Chem. Lett.* **2012**, *3*, 3599 – 3604.

[20] a) F.-R. Fan, Z.-Q. Tian, Z. L. Wang, *Nano Energy* **2012**, *1*, 328 – 334; b) G. Zhu, Z.-H. Lin, Q. Jing, P. Bai, C. Pan, Y. Yang, Y. Zhou, Z. L. Wang, *Nano Lett.* **2013**, *13*, 847 – 853.

[21] L. S. McCarty, G. M. Whitesides, *Angew. Chem.* **2008**, *120*, 2218 – 2239; *Angew. Chem. Int. Ed.* **2008**, *47*, 2188 – 2207.

[22] F.-R. Fan, L. Lin, G. Zhu, W. Wu, R. Zhang, Z. L. Wang, *Nano Lett.* **2012**, *12*, 3109 – 3114.

[23] G. Zhu, C. Pan, W. Guo, C.-Y. Chen, Y. Zhou, R. Yu, Z. L. Wang, *Nano Lett.* **2012**, *12*, 4960 – 4965.

[24] S. Wang, L. Lin, Z. L. Wang, *Nano Lett.* **2012**, *12*, 6339 – 6346.

[25] K. C. Grabar, R. G. Freeman, M. B. Hommer, M. J. Natan, *Anal. Chem.* **1995**, *67*, 735 – 743.

[26] Z.-H. Lin, I.-C. Chen, H.-T. Chang, *Chem. Commun.* **2011**, *47*, 7116 – 7118.

[27] C. A. Mirkin, R. L. Letsinger, R. C. Mucic, J. J. Storhoff, *Nature* **1996**, *382*, 607 – 609.

[28] S. Mann, W. Shenton, M. Li, S. Connolly, D. Fitzmaurice, *Adv. Mater.* **2000**, *12*, 147 – 150.

[29] C.-C. Huang, H.-T. Chang, *Chem. Commun.* **2007**, 1215 – 1217.

[30] Y. Kim, R. C. Johnson, J. T. Hupp, *Nano Lett.* **2001**, *1*, 165 – 167.

[31] A. F. Diaza, R. M. Felix-Navarro, *J. Electrost.* **2004**, *62*, 277 – 290.

[32] J. Zhong, Q. Zhong, F. Fan, Y. Zhang, S. Wang, B. Hu, Z. L. Wang, J. Zhou, *Nano Energy* **2013**, DOI: 10.1016/j.nanoen.2012.11.015.

[33] C.-Y. Liu, A. J. Bard, *Nat. Mater.* **2008**, *7*, 505 – 509.

[34] F. M. M. Morel, *Principles of Aquatic Chemistry*, Wiley-Interscience, New York, **1983**, pp. 248 – 249.

[35] K. Saha, S. S. Agasti, C. Kim, X. Li, V. M. Rotello, *Chem. Rev.* **2012**, *112*, 2739 – 2779.

Communications

Triboelectric Nanosensors

Z.-H. Lin, G. Zhu, Y. S. Zhou, Y. Yang, P. Bai, J. Chen, Z. L. Wang* _____ ▮▮▮▮–▮▮▮▮

A Self-Powered Triboelectric Nanosensor for Mercury Ion Detection

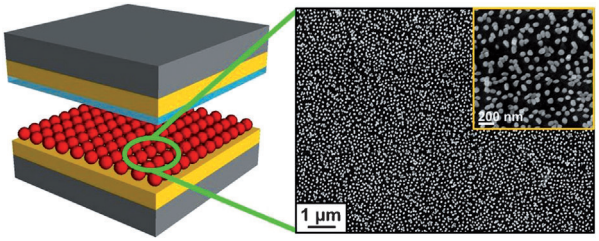

Moving to mercury: The first triboelectric effect-based sensor for the detection of Hg^{2+} ions by using Au nanoparticles (see picture; red) as electrical performance enhancer and recognition element has been successfully demonstrated. This self-powered and stand-alone triboelectric nanosensor has the advantages of simplicity, low cost, high selectivity, and sensitivity.